International Journal of Heat and Mass Transfer 52 (2009) 5040–5045

Contents lists available at ScienceDirect

International Journal of Heat and Mass Transfer

journal homepage: www.elsevier.com/locate/ijhmt

Frequency response and spatial resolution of a thin foil for heat transfer measurements using infrared thermography

Hajime Nakamura *

Department of Mechanical Engineering, National Defense Academy, 1-10-20 Hashirimizu, Yokosuka, Kanagawa 239-8686, Japan

ARTICLE INFO

Article history:
Received 22 October 2008
Accepted 15 April 2009
Available online 24 June 2009

Keywords:
Convective heat transfer
Frequency response
Spatial resolution
Thin foil
Infrared thermography

ABSTRACT

A technique for measuring the spatio-temporal distribution of convective heat transfer has been developed using a test surface fabricated from a thin foil heated electrically. If the heat capacity of the test surface is sufficiently low, the fluctuating temperature on the foil can be measured using high-frame-rate infrared thermography. This method, however, has an inherent problem in that the temperature on the test surface attenuates both in time and space due to thermal inertia and conduction. In the present study, the frequency response and the spatial resolution of a thin foil were examined analytically considering heat losses. In order to derive general relationships, non-dimensional variables of fluctuating frequency and spatial wavenumber were introduced to formulate the temporal and spatial amplitudes of the temperature on the test surface. Based on these relationships, the upper limits on the detectable fluctuating frequency and spatial wavenumber were successfully formulated using governing parameters of the measurement system. This enables us to evaluate quantitatively the reliability of the heat transfer measurement by infrared thermography. The values, evaluated here for the practical conditions, indicated that this measurement technique is promising for investigating the spatio-temporal behavior of heat transfer caused by flow turbulence.

1. Introduction

Convective heat transfer is, by nature, generally nonuniform and unsteady, a fact reflected by three-dimensional flow near a wall. However, most experimental studies concerning convective heat transfer have been performed in a time-averaged manner or using one-point measurements. This frequently results in poor understanding of the heat transfer mechanisms.

Measurement techniques for the temporal and spatial characteristics of heat transfer have been developed using liquid crystals [1] or using infrared thermography [2,3], by employing a thin test surface having a low heat capacity. However, the major problem with these measurements is attenuation and phase delay of the temperature fluctuation due to thermal inertia of the test surface. This becomes serious for higher fluctuating frequencies, for which the fluctuation amplitude weakens and ultimately becomes indistinguishable from noise. In addition, lateral conduction through the test surface attenuates the amplitude of the spatial temperature distribution. This becomes serious for smaller wavelength (higher wavenumber). Therefore, it is important to know both the upper limits of the fluctuating frequency and the spatial wavenumber detectable by the measurement.

In this study, the frequency response and the spatial resolution of a thin foil for heat transfer measurement were examined analytically considering heat losses. In order to derive general relationships, non-dimensional variables of fluctuating frequency and spatial wavenumber were introduced to formulate the amplitude of temperature fluctuation and/or distribution on the test surface. Based on these relationships, the upper limits on the detectable fluctuating frequency and spatial wavenumber were successfully formulated as a function of the temperature resolution (noise-equivalent temperature difference) of infrared measurements for a blackbody.

2. Governing equations

Fig. 1 shows a schematic model for heat transfer measurement. The test surface, which is exposed to air flow, is fabricated from a thin metallic foil (thickness δ, specific heat c, density ρ, thermal conductivity λ, and total emissivity ε_t). An instantaneous temperature distribution and its fluctuation on the test surface can be measured using infrared thermography through the air-stream, which is transparent for infrared radiation. Inside the foil, there is a high-conductivity plate (total emissivity ε_{tc}) to impose a thermal boundary condition of a steady and uniform temperature. Between the foil and the high-conductivity plate is some material of low conductivity and low heat capacity, such as still air, forming an

* Tel.: +81 46 841 3810x3419; fax +81 46 844 5900.
E-mail address: nhajime@nda.ac.jp

0017-9310/$ - see front matter © 2009 Elsevier Ltd. All rights reserved.
doi:10.1016/j.ijheatmasstransfer.2009.04.019

Nomenclature

b	wavelength of spatial distribution (m)
c	specific heat (J/kg K)
f, f_c	frequency, cut-off frequency (Hz)
h	heat transfer coefficient (W/m^2 K)
h_t	total heat transfer coefficient including conduction and radiation (W/m^2 K)
k	wavenumber = $2\pi/b$ (m^{-1})
$\dot{q}$	heat flux (W/m^2)
T	temperature (K)
T_0, T_w	free stream temperature, wall temperature (K)
ΔT_{IR}	temperature resolution of infrared thermography for a non-blackbody (K)
ΔT_{IRO}	noise-equivalent temperature difference of infrared thermography for a blackbody (K)
t	time (s)
x, y, z	tangential, normal and spanwise coordinates
α	thermal diffusivity = $\lambda/c\rho$ (m^2/s)
β	space resolution (m)
δ	thickness (m)
ε_t	total emissivity
ε_{IR}	spectral emissivity for infrared thermograph
κ	$=\sqrt{\omega/2\alpha}$ (m^{-1})
λ	thermal conductivity of fluid (W/m K)
ν	kinematic viscosity (m^2/s)
ρ	density (kg/m^3)
τ	time constant (s)
ω	angular frequency = $2\pi f$ (rad/s)

Subscripts

c, i	high-conductivity plate, insulating layer
cd, cv, rd	conduction, convection, radiation
f, s	frequency response, space resolution

Superscripts

$\bar{(\cdot)}$	time- or space-averaged value
$\tilde{(\cdot)}$	non-dimensional value
$(\cdot)^*$	effective value

insulating layer (thickness δ_i, specific heat c_i, density ρ_i, thermal conductivity λ_i).

The tangential and normal directions with respect to the test surface correspond to x and y coordinates, respectively. Assuming that the temperature is uniform along its thickness and in the spanwise (z) direction, the heat balance on the thin foil can be expressed as:

$$c\rho\delta\frac{\partial T_w}{\partial t}=\lambda\delta\frac{\partial^2 T_w}{\partial x^2}+\dot{q}\quad(y=0). \tag{1}$$

Here, T_w is local and instantaneous temperature of the thin foil. The heat flux, $\dot{q}$, is given by

$$\dot{q}=\dot{q}_{in}-\dot{q}_{cv}-\dot{q}_{cd}-\dot{q}_{rd}-\dot{q}_{rdi}, \tag{2}$$

where $\dot{q}_{in}$ is the input heat flux to the thin foil due to Joule heating, $\dot{q}_{cv}$ and $\dot{q}_{cd}$ are heat fluxes from the thin foil due to convection and conduction, respectively, and $\dot{q}_{rd}$ is radiation heat flux to outside the foil. If the insulating layer is transparent for infrared radiation, as is air, radiation heat flux $\dot{q}_{rdi}$ occurs to the inside. The above heat fluxes are expressed as follows:

$$\dot{q}_{cv}=h(T_w-T_0) \tag{3}$$

$$\dot{q}_{cd}=-\lambda_i\left(\frac{dT}{dy}\right)_{y=0+} \tag{4}$$

$$\dot{q}_{rd}=\varepsilon_t\sigma(T_w^4-T_0^4) \tag{5}$$

$$\dot{q}_{rdi}=\frac{\sigma(T_w^4-T_c^4)}{1/\varepsilon_t+1/\varepsilon_{tc}-1} \tag{6}$$

Here, h is the heat transfer coefficient due to convection to the stream outside, T_0 is the free stream temperature, T_c is surface temperature of the high-conductivity plate, and σ is the Stefan–Boltzmann constant.

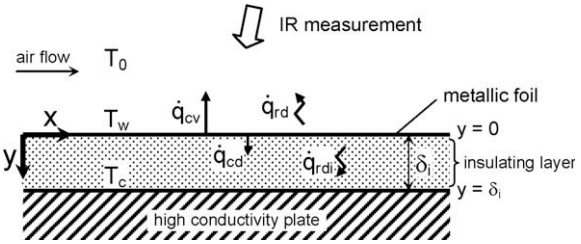

Fig. 1. Schematic model for measurement of heat transfer to air.

Heat conduction in the insulating layer is expressed as:

$$c_i\rho_i\frac{\partial T}{\partial t}=\lambda_i\left(\frac{\partial^2 T}{\partial x^2}+\frac{\partial^2 T}{\partial y^2}\right)\quad(0<y<\delta_i). \tag{7}$$

The frequency response and the spatial resolution of T_w for the heat transfer to the free stream can be calculated using Eqs. (1)–(7) for arbitrary changes in the heat transfer coefficient in time and space.

3. Analytical solutions without heat losses

3.1. Time constant

Assuming that the temperature is uniform in the x direction, and that heat conduction $\dot{q}_{cd}$ and radiation $\dot{q}_{rd}$ and $\dot{q}_{rdi}$ are sufficiently small, Eqs. (1)–(3) yield the following differential equation:

$$c\rho\delta\frac{\partial T_w}{\partial t}=\dot{q}_{in}-h(T_w-T_0). \tag{8}$$

Solving Eq. (8) yields the time constant τ, which is expressed as:

$$\tau=\frac{c\rho\delta}{h}. \tag{9}$$

3.2. Spatial resolution

Assuming that the temperature on the test surface is steady and has a sinusoidal distribution in the x direction, then:

$$T_w=\overline{T}_w+\Delta T_w\sin\left(\frac{2\pi}{b}x\right), \tag{10}$$

where $\overline{T}_w$ and ΔT_w are the mean and spatial amplitude of the temperature of the thin foil, respectively, and b is the wavelength. If $\dot{q}_{cd}$, $\dot{q}_{rd}$ and $\dot{q}_{rdi}$ are sufficiently small, Eqs. (1)–(3) yield the following equation:

$$h(T_w-T_0)=\dot{q}_{cv}=\dot{q}_{in}+\lambda\delta\frac{d^2T_w}{dx^2}. \tag{11}$$

If the thin foil is thermally insulated, Eq. (11) reduces to:

$$h(T_{w0}-T_0)=\dot{q}_{cv}=\dot{q}_{in}. \tag{12}$$

Then, the temperature of the insulated surface T_{w0} is calculated from Eqs. (10)–(12) as

$$T_{w0} = \overline{T}_w + \left\{\frac{\lambda\delta}{h}\left(\frac{2\pi}{b}\right)^2 + 1\right\}\Delta T_w \sin\left(\frac{2\pi}{b}x\right). \tag{13}$$

A comparison between Eqs. (10) and (13) yields the attenuation rate of the spatial amplitude due to lateral conduction through the thin foil:

$$\xi = \frac{1}{\frac{\lambda\delta}{h}\left(\frac{2\pi}{b}\right)^2 + 1}. \tag{14}$$

A spatial resolution β can be defined as the wavelength b at which the attenuation rate is 1/2:

$$\beta = b_{(\xi=1/2)} = 2\pi\sqrt{\frac{\lambda\delta}{h}}. \tag{15}$$

Incidentally, if the test surface has a two-dimensional temperature distribution such as:

$$T_w = \overline{T}_w + \Delta T_w \sin\left(\frac{2\pi}{b}x\right)\sin\left(\frac{2\pi}{b}z\right), \tag{16}$$

then the spatial resolution can be calculated as:

$$\beta_{2D} = 2\pi\sqrt{\frac{2\lambda\delta}{h}}. \tag{17}$$

This indicates that the spatial resolution for the 2D temperature distribution deteriorates by a factor of $\sqrt{2}$.

4. General relations considering heat losses

4.1. Frequency response

Assuming that the temperature on the thin foil is uniform and fluctuates sinusoidally in time, then:

$$T_w = \overline{T}_w + \Delta T_w \sin(\omega t). \tag{18}$$

According to the solution of Carslaw and Jaeger [4], the temperature in the slab ($0 < y < \delta_i$) with zero initial temperature and $T = \sin(\omega t)$ at $y = 0$ and $T = 0$ at $y = \delta_i$ is expressed as follows:

$$T = A\sin(\omega t + \phi)$$
$$A = \left|\frac{\sinh\kappa_i y(1+i)}{\sinh\kappa_i\delta_i(1+i)}\right|, \quad \phi = \arg\left\{\frac{\sinh\kappa_i y(1+i)}{\sinh\kappa_i\delta_i(1+i)}\right\}, \quad \kappa_i = \sqrt{\frac{\omega}{2\alpha_i}} \tag{19}$$

Here, | | and arg{} denote the absolute value and the argument of a complex number, respectively, and α_i is thermal diffusivity of the insulating layer.

Based on Eq. (19), the vertical temperature distribution in the insulating layer, given by $T = \overline{T}_w + \Delta T_w \sin(\omega t)$ at $y = 0$ and $\overline{T}_c$ at $y = \delta_i$ with initial temperature $T = \overline{T}_w(\overline{T}_c - \overline{T}_w)y/\delta_i$ (linear distribution), is expressed as follows by superposition:

$$T = \overline{T}_w + \Delta T_w A\sin(\omega t + \phi) + (\overline{T}_c - \overline{T}_w)y/\delta_i \tag{20}$$

Fig. 2 shows the instantaneous temperature distribution in the insulating layer at $\omega t = \pi/2$, at which the temperature of the thin foil ($y = 0$) is maximum. The shape of the distribution depends only on $\kappa_i\delta_i$. For lower frequencies ($\kappa_i\delta_i < 1$), the distribution can be assumed linear, while for higher frequencies ($\kappa_i\delta_i >> 1$), the temperature fluctuates only in the vicinity of the foil ($y/\delta_i < 1/\kappa_i\delta_i$).

Introducing the effective thickness of the insulating layer, $(\delta_i^*)_f$, the temperature of which fluctuates with the thin foil:

$$(\delta_i^*)f \approx 0.5\delta_i \quad (\kappa_i\delta_i < 1) \tag{21}$$
$$(\delta_i^*)f \approx 0.5/\kappa_i \quad (\kappa_i\delta_i >> 1). \tag{22}$$

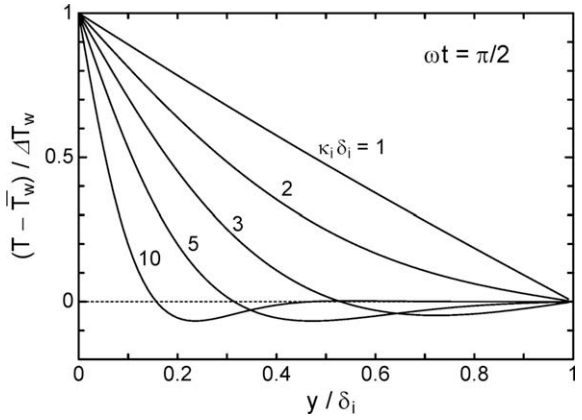

Fig. 2. Instantaneous temperature distribution in the insulating layer at $\omega t = \pi/2$ and $\overline{T}_w = \overline{T}_c$.

The heat capacity of this region works as an additional heat capacity that deteriorates the frequency response. Thus, the effective time constant can be defined as:

$$\tau^* \approx \frac{c\rho\delta + c_i\rho_i(\delta_i^*)_f}{h_t}, \tag{23}$$

$$h_t = \frac{\dot{q}_{in}}{T_w - T_0}. \tag{24}$$

Here, h_t is total heat transfer coefficient from the thin foil, including the effects of conduction and radiation. Then, the cut-off frequency is defined as follows:

$$f_c^* = \frac{1}{2\pi\tau^*}. \tag{25}$$

We introduce the following non-dimensional frequency and non-dimensional amplitude of the temperature fluctuation:

$$\tilde{f} = f/\overline{f}_c^* \tag{26}$$

$$(\Delta\tilde{T}_w)_f = \frac{(\Delta T_w)_f}{\overline{T}_w - T_0}\frac{\overline{h}_t}{\Delta h}. \tag{27}$$

Here, $(\Delta\tilde{T}_w)_f$ includes the factor $\overline{h_t}/\Delta h$ to extend the value of $(\Delta\tilde{T}_w)_f$ to unity at the lower frequency in the absence of conductive or radiative heat losses (see Fig. 3).

Next, we attempt to obtain the relation between $\tilde{f}$ and $(\Delta\tilde{T}_w)_f$. The fluctuating amplitude of the surface temperature, $(\Delta T_w)_f$, can be determined by solving the heat conduction equations of Eqs. (1) and (7) by the finite difference method assuming a uniform temperature in the x direction. The boundary condition on the foil

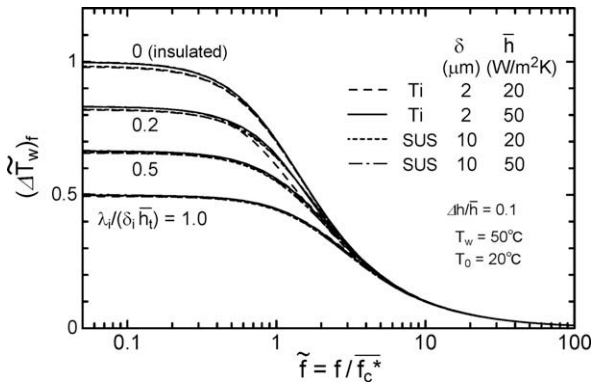

Fig. 3. Relation between non-dimensional frequency $\tilde{f}$ and non-dimensional fluctuating amplitude $(\Delta\tilde{T}_w)_f$.

($y = 0$) is given by the heat transfer coefficient which fluctuates sinusoidally [$h = \overline{h} + \Delta h \sin(\omega t)$]. Fig. 3 plots the relation of $(\Delta\tilde{T}_w)_f$ versus $\tilde{f}$ for practical conditions [5,6]. The thin foil is fabricated from a titanium foil 2 μm thick ($c\rho\delta = 4.7$ J/m^2 K, $\lambda\delta = 32$ μW/K, $\varepsilon_{IR} = 0.183$) or a stainless-steel foil 10 μm thick ($c\rho\delta = 40$ J/m^{2}K, $\lambda\delta = 160$ μW/K, $\varepsilon_{IR} = 0.15$), the insulating layer is a still air layer without convection, and the mean heat transfer coefficient is $\overline{h} = 20$–50 W/m^2 K. Since the amplitude of the heat transfer coefficient Δh is almost independent of the relation if it is not too high, the value is tentatively set to $\Delta h/\overline{h} = 0.1$. A parameter of $\lambda_i/(\delta_i\overline{h}_t)$, which represents the effect of conduction from the foil to the high-conductivity plate through the insulating layer, is varied from 0 to 1.

For the lower frequency of $\tilde{f} < 0.1$, $(\Delta\tilde{T}_w)_f$ approaches a constant value:

$$(\Delta\tilde{T}_w)_f \approx \frac{1}{1 + \lambda_i/(\delta_i\overline{h}_t)} \quad (\tilde{f} < 0.1). \tag{28}$$

In this case, the fluctuating amplitude decreases with increasing $\lambda_i/(\delta_i\overline{h}_t)$. For higher frequency values of $\tilde{f} > 4$, the value of $(\Delta\tilde{T}_w)_f$ depends only on $\tilde{f}$. Consequently, it simplifies to a single relation (within ±3% for the present conditions):

$$(\Delta\tilde{T}_w)_f \approx \frac{1}{\tilde{f}} \quad (\tilde{f} > 4). \tag{29}$$

4.2. Spatial resolution

Assuming that the temperature on the foil is steady and has a sinusoidal temperature distribution in the x direction, then:

$$T_w = \overline{T}_w + \Delta T_w \sin(kx), \quad k = 2\pi/b. \tag{30}$$

Here, k is wavenumber of the spatial distribution.

The steady temperature in the rectangle ($0 < y < \delta_i$, $0 < x < b$), with temperature distribution of $T = \sin(kx)$ at $y = 0$ and $T = 0$ at $y = \delta_i$ is expressed as follows [4]:

$$T = \sin(kx)\sinh(k(\delta_i - y))\mathrm{cosech}(k\delta_i) \tag{31}$$

Based on Eq. (31), the temperature distribution in the insulating layer, given by $\overline{T}_w + \Delta T_w \sin(kx)$ at $y = 0$ and $\overline{T}_c$ at $y = \delta_i$, is expressed as follows by superposition:

$$T = \overline{T}_w + \Delta T_w \sin(kx)\sinh(k(\delta_i - y))\mathrm{cosech}(k\delta_i) + (\overline{T}_c - \overline{T}_w)y/\delta_i \tag{32}$$

Fig. 4 shows the vertical temperature distribution in the insulating layer at $kx = \pi/2$, at which the temperature of the thin foil ($y = 0$) is maximum. The shape of the distribution depends only on $k\delta_i$. For the lower wavenumber ($k\delta_i < 1$), the distribution can be assumed linear, while for the higher wavenumber ($k\delta_i >> 1$), the distribution approaches an exponential function.

Now, we introduce an effective thickness of the insulating layer, $(\delta_i^*)_s$, the temperature of which is affected by the temperature distribution on the foil:

$$(\delta_i^*)_s \approx \delta_i \quad (k\delta_i < 1) \tag{33}$$

$$(\delta_i^*)_s \approx 1/k \quad (k\delta_i >> 1) \tag{34}$$

[The thickness $(\delta_i^*)_s$ was defined here so as to formulate the non-dimensional relationship between $\tilde{k}$ and $(\Delta\tilde{T}_w)_s$ (see below). The physical reason for the difference in the form from $(\delta_i^*)_f$ (see Eqs. (21) and (22)) is not clear at present.] The heat conduction of this region functions as an additional heat spreading parameter that reduces the spatial resolution. Thus, the effective spatial resolution can be defined as:

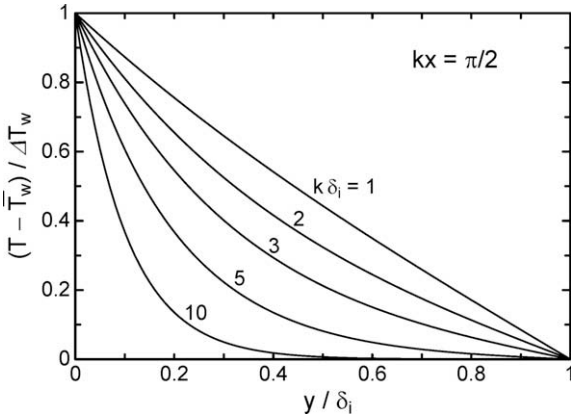

Fig. 4. Temperature distribution in the insulating layer at $kx = \pi/2$ and $\overline{T}_w = \overline{T}_c$.

$$\beta^* \approx 2\pi\sqrt{\frac{\lambda\delta + \lambda_i(\delta_i^*)_s}{h_t}}. \tag{35}$$

Introduce a non-dimensional wavenumber and non-dimensional amplitude of the spatial temperature distribution:

$$\tilde{k} = \frac{k}{(2\pi/\overline{\beta}^*)} = \frac{k\overline{\beta}^*}{2\pi} \tag{36}$$

$$(\Delta\tilde{T}_w)_s = \frac{(\Delta T_w)_s}{\overline{T}_w - T_0}\frac{\overline{h}_t}{\Delta h}. \tag{37}$$

Here, $2\pi/\overline{\beta}^*$ corresponds to the cut-off wavenumber.

Next, we attempt to obtain a relation between $\tilde{k}$ and $(\Delta\tilde{T}_w)_s$. The spatial amplitude of the surface temperature, $(\Delta T_w)_s$, can be determined by solving a steady-state solution of the heat conduction equations of Eqs. (1) and (7) by the finite difference method. The boundary condition on the foil ($y = 0$) is given by the sinusoidal distribution of the heat transfer coefficient along x [$h = \overline{h} + \Delta h \sin(kx)$]. Fig. 5 plots the relation of $(\Delta\tilde{T}_w)_s$ versus $\tilde{k}$ for practical conditions (see Section 4.1). For the lower wavenumber of $\tilde{k} < 0.1$, $(\Delta\tilde{T}_w)_s$ approaches a constant value of

$$(\Delta\tilde{T}_w)_s \approx \frac{1}{1 + \lambda_i/(\delta_i\overline{h}_t)} \quad (\tilde{k} < 0.1). \tag{38}$$

In this case, the spatial amplitude decreases with increasing $\lambda_i/(\delta_i\overline{h}_t)$, which represents the heat conduction loss to the high-conductivity plate. For the higher wavenumber of $\tilde{k} > 4$ the value of $(\Delta\tilde{T}_w)_s$ depends only on $\tilde{k}$. It, therefore, corresponds to a single relation (within ±3% for the present conditions).

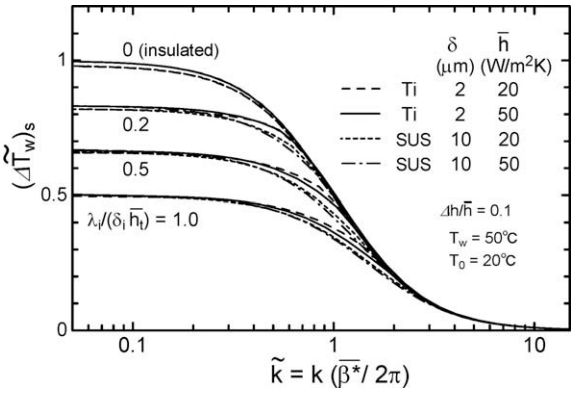

Fig. 5. Relation between non-dimensional wavenumber $\tilde{k}$ and non-dimensional spatial amplitude $(\Delta\tilde{T}_w)_s$.

$$(\Delta\tilde{T}_w)_s \approx \frac{1}{\tilde{k}^2} \quad (\tilde{k} > 4) \tag{39}$$

5. Detectable limits for infrared thermography

5.1. Temperature resolution

The present measurement is feasible if the amplitude of the temperature fluctuation, $(\Delta T_w)_f$, and the amplitude of the spatial temperature distribution, $(\Delta T_w)_s$, is greater than the temperature resolution of infrared measurement, ΔT_{IR}. In general, the temperature resolution of a product is specified as a value of noise-equivalent temperature difference (NETD) for a blackbody, ΔT_{IR0}.

The spectral emissive power detected by infrared thermograph, E_{IR}, can be assumed as follows:

$$E_{IR}(T) = \varepsilon_{IR} C T^n, \tag{40}$$

where ε_{IR} is spectral emissivity for infrared thermograph, and C and n are constants which depend on wavelength of infrared radiation and so forth. For a blackbody, the noise amplitude of the emissive power can be expressed as follows:

$$\Delta E_{IR0}(T) = C(T + \Delta T_{IR0})^n - CT^n \tag{41}$$

Similarly, for a non-blackbody, the noise amplitude can be expressed as follows:

$$\Delta E_{IR}(T) = \varepsilon_{IR} C(T + \Delta T_{IR})^n - \varepsilon_{IR} CT^n \tag{42}$$

Since the noise intensity is independent of spectral emissivity ε_{IR}, the values of $\Delta E_{IR0}(T)$ and $\Delta E_{IR}(T)$ are identical. This yields the following relation using the binomial theorem with the assumption of $T >> \Delta T_{IR0}$ and $T >> \Delta T_{IR}$.

$$\Delta T_{IR} = \Delta T_{IR0}/\varepsilon_{IR} \tag{43}$$

Namely, the temperature resolution for a non-blackbody is inversely proportional to ε_{IR}.

5.2. Upper limit of fluctuating frequency

Using Eqs. (22)–(27) and (29), the fluctuating amplitude, $(\Delta T_w)_f$, is generally expressed as follows for higher fluctuating frequency:

$$(\Delta T_w)_f \approx \frac{(\overline{T}_w - T_0)\Delta h}{2\pi c\rho\delta f + \sqrt{\pi c_i \rho_i \lambda_i} f^{0.5}}, \quad (\tilde{f} > 4 \quad \text{and} \quad k_i\delta_i >> 1) \tag{44}$$

The fluctuation is detectable using infrared thermography for $(\Delta T_w)_f > \Delta T_{IR}$. This yields the following equation from Eqs. (43) and (44).

$$f < \left(\frac{-B + \sqrt{B^2 - 4AC}}{2A}\right)^2 \tag{45}$$

$$A = 2\pi c\rho\delta, \quad B = \sqrt{\pi c_i \rho_i \lambda_i}, \quad C = -\varepsilon_{IR}\Delta h(\overline{T}_w - T_0)/\Delta T_{IR0}$$

The maximum frequency of Eq. (45) at $(\Delta T_w)_f = \Delta T_{IR}$ corresponds to the upper limit of the detectable fluctuating frequency, f_{max}. The value of f_{max} is uniquely determined as a function of $\Delta h(\overline{T}_w - T_0)/\Delta T_{IR0}$ if the thermophysical properties of the thin foil and the insulating layer are specified.

Fig. 6 shows the relation of f_{max} for practical metallic foils for heat transfer measurement to air, namely, a titanium foil of 2 μm thick ($c\rho\delta$ = 4.7 J/m^2 K, ε_{IR} = 0.183) and a stainless-steel foil of 10 μm thick ($c\rho\delta$ = 40 J/m^2 K, ε_{IR} = 0.15). Also, the relation of the carbon film of 5 μm thickness ($c\rho\delta$ = 6.8 J/m^2 K, ε_{IR} = 0.6), which was tested in Ref. [7], is plotted because of its higher frequency response and spatial resolution, although it has some defects in practical use at present. The insulating layer is assumed to be a still air layer (c_i = 1007 J/kg K, ρ_i = 1.18 kg/m^3, λ_i = 0.0265 W/m K), which has low heat capacity and thermal conductivity.

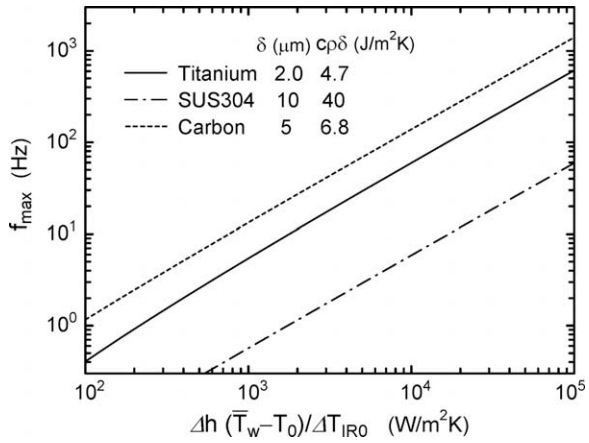

Fig. 6. Upper limit of the fluctuating frequency detectable using infrared measurements.

For example, a practical condition likely to appear in flow of low-velocity turbulent air [6] ($\Delta h(\overline{T}_w - T_0)/\Delta T_{IR0} = 6000$ W/m^2 K; Δh = 5 W/m^2 K, $\overline{T}_w - T_0$ = 30 K, and ΔT_{IR0} = 0.025 K), gives the values f_{max} = 35 Hz for the 2 μm thick titanium foil and f_{max} = 83 Hz for the 5 μm thick carbon film. Therefore, the unsteady heat transfer caused by flow turbulence can be detected using this measurement technique, although it may be limited to fluctuations due to large-scale structure, as suggested in Ref. [6].

The value of f_{max} increases with decreasing $c\rho\delta$ and ΔT_{IR0}, and with increasing ε_{IR}, Δh, and $\overline{T_w} - T_0$. The improvements of both the infrared thermograph (decreasing ΔT_{IR0} with increasing frame rate) and the thin foil (decreasing $c\rho\delta$ and/or increasing ε_{IR}) will improve the measurement.

5.3. Upper limit of spatial wavenumber

Using Eqs. (34)–(37) and (39), the spatial amplitude, $(\Delta T_w)_s$, is generally expressed as follows for higher wavenumber:

$$(\Delta T_w)_s \approx \frac{(\overline{T}_w - T_0)\Delta h}{\lambda\delta k^2 + \lambda_i k}, \quad (\tilde{k} > 4 \quad \text{and} \quad k\delta_i >> 1). \tag{46}$$

The spatial distribution is detectable using infrared thermography for $(\Delta T_w)_s > \Delta T_{IR}$. This yields the following equation using Eqs. (43) and (46).

$$k < \frac{-\lambda_i + \sqrt{\lambda_i^2 + 4\lambda\delta\varepsilon_{IR}\{\Delta h(\overline{T}_w - T_0)/\Delta T_{IR0}\}}}{2\lambda\delta} \tag{47}$$

The maximum wavenumber of Eq. (47) at $(\Delta T_w)_f = \Delta T_{IR}$ corresponds to the upper limit of the detectable spatial wavenumber, k_{max}. If thermophysical properties of the thin foil and the insulating layer are specified, the value of k_{max} is uniquely determined as a function of $\Delta h(\overline{T}_w - T_0)/\Delta T_{IR0}$, as well as f_{max}.

Fig. 7 shows the relation for k_{max} for the titanium foil of 2 μm thickness ($\lambda\delta$ = 32 μW/K, ε_{IR} = 0.183), the stainless-steel foil of 10 μm thickness ($\lambda\delta$ = 160 μW/K, ε_{IR} = 0.15), and the carbon film of 5 μm thickness ($\lambda\delta$ = 6.5 μW/K, ε_{IR} = 0.6). The insulating layer is assumed to be a still air layer (λ_i = 0.0265 W/m K). For example, at $\Delta h(\overline{T}_w - T_0)/\Delta T_{IR0} = 6000$ W/m^2 K [6], the value of k_{max} (b_{min}) is 5.5 mm^{-1} (1.2 mm) for the 2 μm thick titanium foil, and 22 mm^{-1} (0.3 mm) for the 5 μm thick carbon film. Therefore, the spatial structure of the heat transfer coefficient caused by flow turbulence can be detected using this measurement technique, although it may be limited to the large-scale structure, as suggested in Ref. [6].

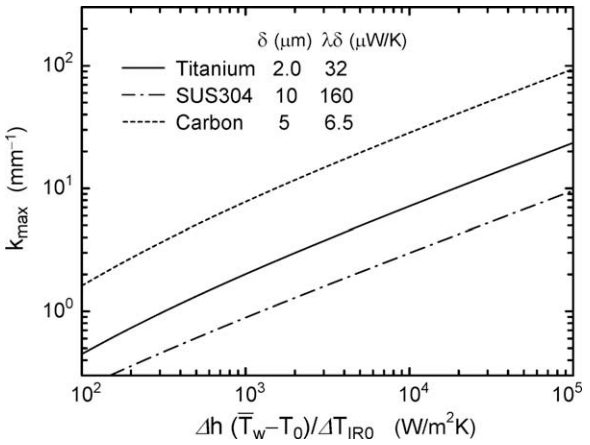

Fig. 7. Upper limit of the spatial wavenumber detectable using infrared measurements.

The value of k_{max} increases with decreasing $\lambda\delta$ and ΔT_{IR0}, and with increasing ε_{IR}, Δh, and $\overline{T}_w\overline{T}_0$. The improvements of both the infrared thermograph (decreasing ΔT_{IR0} with increasing pixel resolution) and the thin foil (decreasing $\lambda\delta$ and/or increasing ε_{IR}) will improve the measurement.

6. Conclusions

The frequency response and the spatial resolution of a thin foil for measurements of the spatio-temporal distribution of convective heat transfer were investigated analytically. The results are summarized as follows:

(1) The time constant τ and the spatial resolution β without heat losses are expressed as follows:

$$\tau = \frac{c\rho\delta}{h}, \quad \beta = 2\pi\sqrt{\frac{\lambda\delta}{h}}.$$

(2) The effective values of the time constant and the spatial resolution, considering heat losses, can be expressed as follows:

$$\tau^* \approx \frac{c\rho\delta + c_i\rho_i(\delta_i^*)_f}{h_t} \quad \begin{matrix}(\delta)_i^*)_f \approx 0.5\delta_i, (\kappa_i\delta_i < 1) \\ (\delta_i^*)_f \approx 0.5/k_i, (\kappa_i\delta_i >> 1)\end{matrix}$$

$$\beta^* \approx 2\pi\sqrt{\frac{\lambda\delta + \lambda_i(\delta_i^*)_s}{h_t}} \quad \begin{matrix}(\delta_i^*)_s \approx \delta_i, (k\delta_i < 1) \\ (\delta_i^*)_s \approx 1/k, (k\delta_i >> 1)\end{matrix}$$

(3) The upper limits of the fluctuating frequency, f_{max}, and the spatial wavenumber, k_{max}, which are detectable using infrared thermography, can be expressed as follows:

$$f_{max} = \left(\frac{-B + \sqrt{B^2 - 4AC}}{2A}\right)^2$$

$$A = 2\pi c\rho\delta, \quad B = \sqrt{\pi c_i\rho_i\lambda_i}, \quad C = -\varepsilon_{IR}\Delta h(\overline{T}_w - T_0)/\Delta T_{IR0}$$

$$k_{max} = \frac{-\lambda_i + \sqrt{\lambda_i^2 + 4\lambda\delta\varepsilon_{IR}\{\Delta h(\overline{T}_w - T_0)/\Delta T_{IR0}\}}}{2\lambda\delta}$$

The values of f_{max} and k_{max} are uniquely determined as functions of $\Delta h(\overline{T}_w - T_0)/\Delta T_{IR0}$, if thermophysical properties of the thin foil (c, ρ, δ, λ, ε_{IR}) and the insulating layer (c_i, ρ_i, λ_i) are specified.

References

[1] Y. Iritani, N. Kasagi, M. Hirata, Heat transfer mechanism and associated turbulent structure in the near-wall region of a turbulent boundary layer, in: 4th Symposium on Turbulent Shear Flows, Karlsruhe, Germany, 1983, pp. 17.31–17.36.
[2] G. Hetsroni, R. Rozenblit, Heat transfer to a liquid–solid mixture in a flume, Int. J. Multiphase Flow 20 (4) (1994) 671–689.
[3] H. Nakamura, T. Igarashi, Unsteady heat transfer from a circular cylinder for Reynolds numbers from 3000 to 15000, Int. J. Heat Fluid Flow 25 (2004) 741–748.
[4] H.S. Carslaw, J.C. Jaeger, Conduction of Heat in Solids, second ed., Oxford University Press, 1959. pp.105–106, pp.166–167.
[5] H. Nakamura, T. Igarashi, A new technique for measurements of unsteady heat transfer to air using a thin metallic-foil and infrared thermograph, in: 13th International Heat Transfer Conference, Sydney, Australia, 2006, EXP-11.
[6] H. Nakamura, Measurements of time–space distribution of convective heat transfer to air using a thin conductive-film, in: 5th International Symposium on Turbulence and Shear Flow Phenomena, München, 2007, pp.773–778.
[7] H. Nakamura, T. Igarashi, Measurements of time–space distribution of convective heat transfer using a thin carbon-film, in: 5th International Symposium on Turbulence, Heat and Mass Transfer, Dubrovnik, Croatia, 2006, pp. 247–250.